Annals of Science and Inquiry
Vol. 2 No. 6 (2026)

A single shear-strength ranking is not identified by a simulant parameter table: stress-support comparisons in an open lunar-regolith compilation

Gregory Franklin[1] · Ethan Hughes[2] · Paul Lewis[3]

[1] Australia · [2] New Zealand · [3] Netherlands

Published: June 17, 2026 | Article 853

Abstract

Cohesion and friction angle describe a stress-dependent line, yet material tables often invite a single ranking. We examined the complete 26-row September 2026 simulant release of the Lunar Regolith Database without treating compiled coefficients as new experiments. Eleven scalar direct-shear rows generated 55 comparisons on their reported shared normal-stress intervals. Twenty-eight lines crossed, 26 maintained strict order, and one pair was identical. Removing one underlying source family changed the crossing fraction from 50.9% to a range of 10.0–60.0%. Converting a source guide's nominal loads instead of using the archive's approximate limits changed one boundary-sensitive classification. Among 36 comparisons involving ranged parameters, 11 lacked common stress support, one had only a common endpoint, and 21 of the remaining 24 had ambiguous order under Cartesian outer envelopes. These finite results expose the conditions required for a parameter-based comparison; they do not establish measured strength differences, an optimal simulant, or lunar operational performance.

A single shear-strength ranking is not identified by a simulant parameter table: stress-support comparisons in an open lunar-regolith compilation

Abstract

Cohesion and friction angle describe a stress-dependent line, yet material tables often invite a single ranking. We examined the complete 26-row September 2026 simulant release of the Lunar Regolith Database without treating compiled coefficients as new experiments. Eleven scalar direct-shear rows generated 55 comparisons on their reported shared normal-stress intervals. Twenty-eight lines crossed, 26 maintained strict order, and one pair was identical. Removing one underlying source family changed the crossing fraction from 50.9% to a range of 10.0-60.0%. Converting a source guide's nominal loads instead of using the archive's approximate limits changed one boundary-sensitive classification. Among 36 comparisons involving ranged parameters, 11 lacked common stress support, one had only a common endpoint, and 21 of the remaining 24 had ambiguous order under Cartesian outer envelopes. These finite results expose the conditions required for a parameter-based comparison; they do not establish measured strength differences, an optimal simulant, or lunar operational performance.

Introduction

A table containing cohesion and friction angle can look like a list of material attributes suitable for sorting. The difficulty is that these two coefficients jointly describe a function of normal stress. A larger cohesion can accompany a smaller friction angle, so neither coefficient alone establishes which predicted shear strength is larger over the conditions of interest. The recently published Lunar Regolith Database makes such comparisons unusually accessible while preserving measurement method and context (Gasteiner et al., 2026a). Its archived release provides an opportunity to ask a narrower question than which simulant best represents the Moon: what ordering is actually supported by the recorded parameter pairs and stress intervals (Gasteiner et al., 2026b)?

The NASA simulant guide illustrates the practical motivation. It compiles cohesion and friction angle alongside other properties and explicitly relates both coefficients to the Mohr-Coulomb envelope (Slabic et al., 2024). Classical soil mechanics treats a failure relation as a model tied to stress conditions, rather than an intrinsic rank detached from loading (Terzaghi, 1943). Constitutive descriptions also distinguish a compact strength relation from the wider evolution of soil state (Wood, 1991). Experimental work on sand connects strength to dilatancy and confinement (Bolton, 1986), while the state-parameter approach combines density and stress information (Been and Jefferies, 1985). Differences between friction and dilatancy angles further caution against treating all reported angles as interchangeable (Schanz and Vermeer, 1996). These considerations motivate a source-conditioned comparison, without requiring new mechanical testing.

The numerical question is concrete. For every eligible pair of source rows, does the difference between the two parameter-implied lines keep the same sign throughout their reported support intersection? A second question asks what can still be concluded when a source reports separate parameter ranges rather than a paired scalar fit. We examine every row in the selected release, preserve missing and conflicting information, and report all eligible scalar comparisons. Our propositions are algebraic and testable in this finite table: opposite endpoint signs identify an interior crossing for scalar affine lines; separate parameter ranges usually provide an outer set of possible comparisons rather than a unique order. The empirical contribution is the extent, distribution and source sensitivity of those outcomes in an actual compilation.

This question also concerns the interpretation of physical inputs supplied to lunar-domain reasoning systems. Lunar-R1 uses continued pretraining, supervised fine-tuning and reinforcement learning, and lists collection and navigation among its application contexts (Xiao et al., 2026). We invoke those contexts only to motivate the need to preserve a physical parameter's conditions when representing information. Lunar-R1 does not report a dedicated evaluation of the soil-mechanics comparisons studied here. We neither run its model nor infer its accuracy from this analysis.

Source and comparison design

The analysis version is the complete September simulant file within version 3.0 of the public archive, released on 6 October 2026 (Gasteiner et al., 2026b). The file contains 26 records and 26 fields. We acquired its 8,027 bytes and matched its archive-supplied MD5 before calculating outcomes. The archive records the Etalab 2.0 licence. A contemporary repository snapshot and the database manual provided documentation; the archived bytes, rather than a moving application view, define the numerical support. The separate 191-row lunar-regolith file and the combined 217-row file were retained for provenance checks, without adding them to the simulant analysis.

The complete audit preserves original row numbers, raw coefficient strings, stress limits, material labels, test methods, source identifiers, environment and comments. There are 14 explicit direct-shear rows, eight triaxial-compression rows and four rows without a stated method. Seven of the 26 lack a reported stress support. One lacks cohesion and another lacks friction angle. These omissions are not replaced with zero. The NAO-1 record contains a numerical cohesion of 95.3 kPa while its comment says that cohesion was assumed zero. We retain both statements and flag their inconsistency; that row is not an eligible direct-shear comparison.

We use the compilation's paired scalar entries for IGG-01 (Ruan et al., 2024), KLS-1 (Ryu et al., 2018), TLS-01 (Seehanam et al., 2021), and the two LHS-1/LMS-1 entries (Yin et al., 2023). These constitute four underlying source families, with the last two materials sharing one study. Six further scalar rows trace to the APL assessment summarized in the NASA guide (Slabic et al., 2024), producing five families in total. Table 19 of that guide independently confirms all six cohesion/angle pairs. The archived OB-1A hyperlink currently provides no numerical shear parameters, whereas the guide supplies the corresponding 15 kPa and 35 degree values. We document that distinction instead of treating every linked page as a successful original-data check. Other numerical rows remain a secondary extraction from the archive unless specifically cross-checked.

The three ranged direct-shear entries are PolyU-1, WHU-1 and EAC-1A. The PolyU-1 study describes multiple direct-shear sets (Zou et al., 2024). The WHU-1 paper explicitly distinguishes loading conditions and reports nonlinear direct-shear response (Teng et al., 2025), which makes a single globally valid line especially inappropriate. Their archive ranges are retained as published inputs to a conditional calculation. We do not assume that one cohesion endpoint and one friction-angle endpoint were obtained together. Triaxial examples such as BP-1 (Suescun-Florez et al., 2015) and JSC-1A (Alshibli and Hasan, 2009) remain in the audit, since a confining-pressure interval cannot silently serve as the normal-stress interval of a direct shear plane.

The design deliberately compares source-row representations under recorded conditions. It does not make the specimens, densities or strength states exchangeable. In particular, the archive explicitly labels the LHS-1 and LMS-1 parameters as residual. Both are included in the complete scalar representation and excluded together in a fixed sensitivity. General accounts of soil behavior emphasize the roles of state and loading history (Mitchell et al., 2025); engineering strength applications require additional information

beyond two coefficients (Duncan et al., 2014). Those limitations apply even when the numerical ordering of two reported lines is unambiguous.

Model and finite estimands

For row i we calculate the parameter-implied relation

$$\tau_i(\sigma) = c_i + \sigma \tan(\varphi_i),$$

with cohesion c, normal stress sigma and implied shear stress tau in kPa, and friction angle phi supplied in degrees and converted to radians for evaluating the tangent. We fit no coefficients. The scalar values are inherited from a compilation of earlier studies, and evaluating the equation creates model outputs rather than new shear observations. Micromechanical stress-dilatancy theory already shows why a simple continuum criterion has limited generality for a granular assembly (Rowe, 1962). Particle-based models (Cundall and Strack, 1979) and simulated shear deformation (Thornton, 2000) represent information that these two coefficients do not contain. Our purpose is to inspect the consequences of the tabulated representation itself.

For two stress supports [L_i,U_i] and [L_j,U_j], the shared support starts at the larger lower endpoint and ends at the smaller upper endpoint. Unknown, empty, singleton and positive-width intersections are separate outcomes. No comparison outside the intersection contributes to the order classification. On a positive-width interval, the line difference is affine. Its two endpoint values therefore suffice to establish strict constant order, an interior crossing, a boundary equality or identical lines. For a crossing, we solve the zero of that difference analytically. The numerical equality tolerance is fixed at 10 to the power of minus ten kPa to handle floating arithmetic; it is not a claim about experimental accuracy.

Figure 1 shows the semantic and mathematical gates. Distinguishing the direct-shear plane from principal-stress descriptions matters because different failure criteria use different representations of stress (Drucker and Prager, 1952). The scalar estimand is the count and fraction of eligible row pairs whose lines cross strictly inside the shared interval. Each row appears in multiple pairs, and six rows share the same underlying assessment. Thus 55 comparisons are not 55 independent experiments. We report neither a binomial standard error nor a population confidence interval.

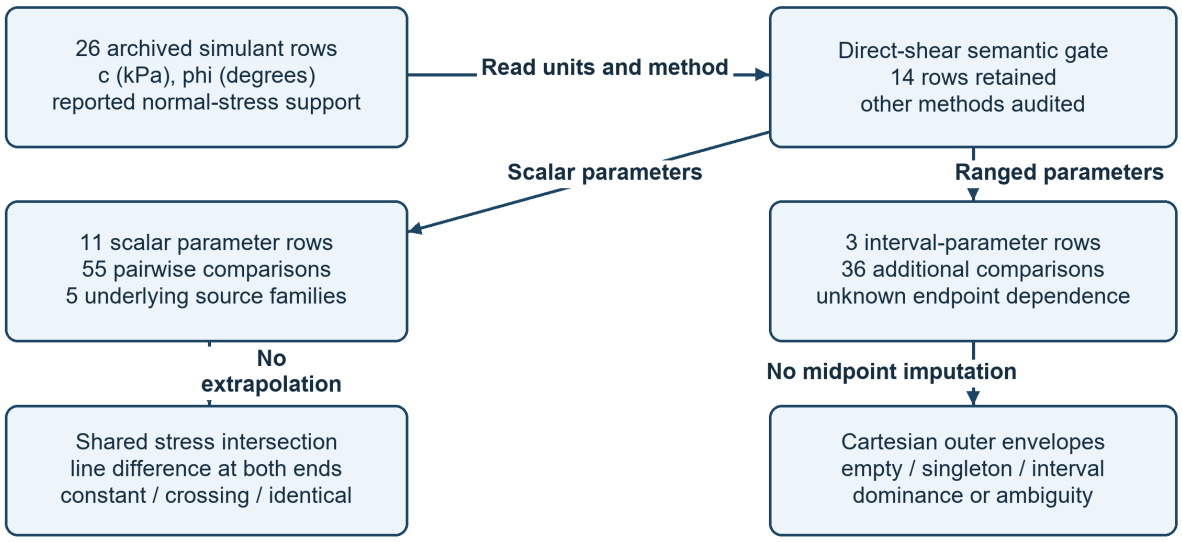

Figure 1. Article-specific comparison model. All 26 source rows remain audited. Eleven scalar rows define 55 primary comparisons; three ranged rows contribute 36 additional comparisons. Arrows describe data transformations and conditional calculations, not physical causal effects.

The fixed source sensitivity deletes each underlying bibliographic family in turn and recomputes the remaining complete pair fraction. Its minimum and maximum are a source-deletion range for this finite table. Geotechnical variability includes distinctions among material variation, measurement error and transformation uncertainty (Phoon and Kulhawy, 1999); our compilation cannot estimate their separate distributions. Reliability analysis requires a defensible uncertainty model (Baecher and Christian, 2003), which a list of repeated source rows cannot supply. Deletion therefore measures dependence on composition of this library, without implying probability coverage.

For an interval-parameter row, the lower outer line uses its lower cohesion and lower angle, while the upper outer line uses the two upper endpoints. Monotonicity of the tangent for the admitted angles and nonnegative normal stress makes those valid Cartesian outer bounds on the specified parameter rectangle. Robust conditional dominance requires one row's lower line to exceed the other's upper line at both support endpoints. Opposite separated outer envelopes at the two ends would force a crossing. Otherwise the outer-set classification is ambiguous. This is an identification exercise in the limited sense that stated information may restrict, without uniquely determining, an answer (Manski, 2003). It does not assign probabilities to parameter combinations, and an outer corner need not be physically attainable.

The analysis rules were recorded after source inspection and before calculating crossings. This is a secondary analysis, not a preregistration. Source deletion and residual-row exclusion were fixed at that stage. A later comparison of the archive's approximate stress limits with the guide's nominal load units prompted an additional, explicitly post-result diagnostic. Sensitivity analysis is useful precisely because an assumption can change a model output (Saltelli et al., 2008); here the changed assumption concerns a source representation, not a newly estimated physical effect.

Results

Table 1 reports every scalar line and its original stress interval. The tangent column is calculated from the reported angle and is dimensionless. The c values are source coefficients; uncertainty about their estimation is unavailable in these scalar records. We therefore provide deterministic support and sensitivity information rather than fabricate sampling uncertainty. The two identical 12 kPa, 36 degree entries remain separate rows because they name different materials, while their equality is visible in the pair classification.

Table 1. Complete primary coefficients and supports: 11 source rows, 11 material labels and five source families; no coefficient SE or CI is supplied by this representation.

Material	c (kPa)	phi (degrees)	tan(phi)	Reported sigma support (kPa)	Recorded source/state
IGG-01	19.20	41.80	0.89410	50-200	Ruan study
TLS-01	6.47	33.92	0.67248	30-250	Seehanam study
KLS-1	1.85	44.91	0.99686	10-200	Ryu study
LHS-1	1.70	40.30	0.84806	25-100	Yin study; residual
LMS-1	3.90	40.50	0.85408	25-100	Yin study; residual
CSM-LHT-1	12.00	32.00	0.62487	23-143	APL via NASA guide
CSM-LMT-1	12.00	36.00	0.72654	23-143	APL via NASA guide
NU-LHT-4M	8.00	38.00	0.78129	23-143	APL via NASA guide
OB-1A	15.00	35.00	0.70021	23-143	APL via NASA guide
OPRH3N	12.00	36.00	0.72654	23-143	APL via NASA guide
OPRL2N	7.00	40.00	0.83910	23-143	APL via NASA guide

All 55 scalar pairs have a positive-width intersection. Twenty-eight cross strictly inside that interval, 26 maintain a strict order, and one has identical parameter lines. The crossing fraction is 50.91%, including the identical pair in the denominator. Crossing stresses span 23.34-168.84 kPa in the literal archive representation. Figure 2 displays every pair, avoiding a selection of visually striking examples. A crossing identifies a change in conditional model order; it does not show that measured specimens exchanged performance during a common experiment.

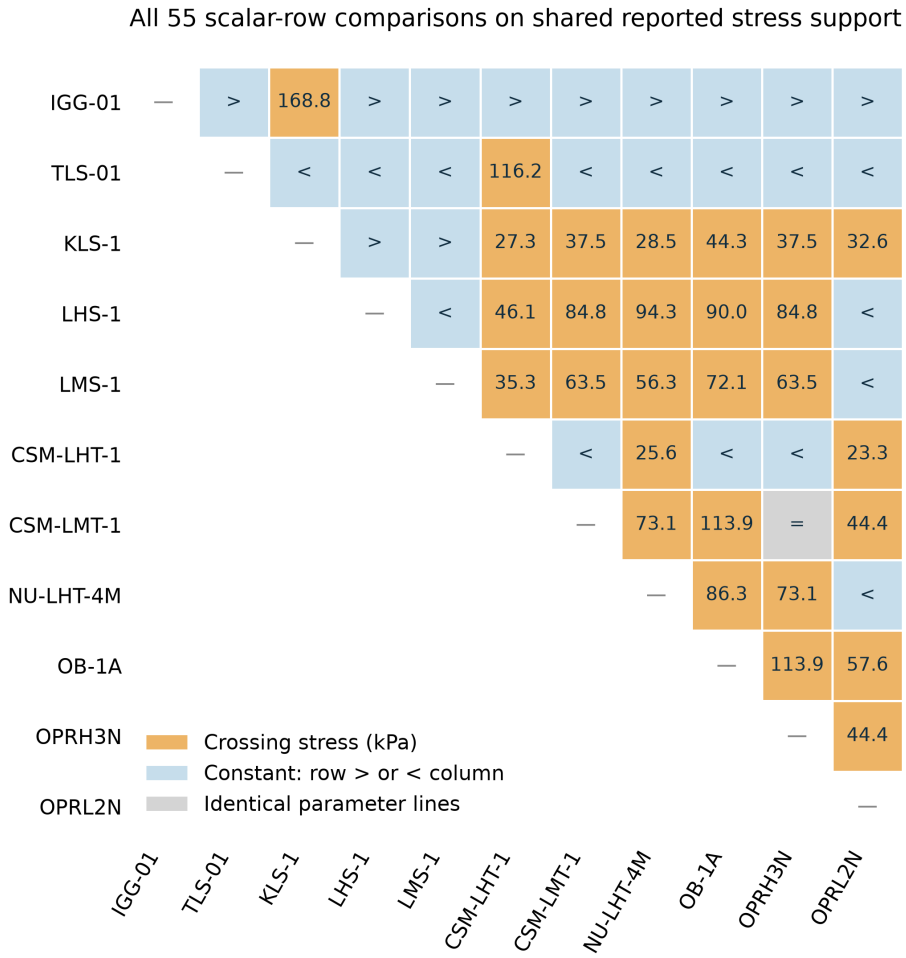

Figure 2. Complete scalar comparison matrix in archive row order. Orange cells give the derived crossing stress to one decimal place; blue inequalities compare the row line with the column line throughout the shared support; grey indicates identical coefficients. Supports differ by pair. Values are conditional model calculations and not measured failure loads or estimates of their uncertainty.

Table 2 reports the finite effects and the uncertainty statements warranted by this source. For IGG-01 minus KLS-1, the predicted contrast changes from +12.21 kPa at the shared lower endpoint of 50 kPa to -3.20 kPa at 200 kPa. This produces the largest interior crossing stress, 168.84 kPa. The sign change is larger than numerical rounding at the displayed endpoints. It still compares different source conditions, so it cannot be interpreted as an experimentally controlled material effect.

Table 2. Actual finite effects and sensitivity. Pair counts describe dependent comparisons of compiled lines; the listed ranges are deterministic, without confidence coverage.

Quantity or fixed diagnostic	Rows / pairs in scope	Result	Uncertainty or support interpretation
Interior crossing fraction	11 / 55	28/55 = 50.91%	Finite table; no sampling CI
Constant strict order	11 / 55	26/55	Conditional on each shared support
Identical parameter lines	11 / 55	1/55	CSM-LMT-1 and OPRH3N
Crossing-stress range	11 / 28 crossing pairs	23.34-168.84 kPa	Deterministic range of derived roots
IGG-01 minus KLS-1 endpoint contrast	2 / 1	+12.21 to -3.20 kPa	At sigma 50 and 200 kPa; different source conditions
Delete one source family	5-10 / 10-45	Crossing fraction 10.00-60.00%	Five source deletions; not a CI
Exclude two explicitly residual rows	9 / 36	18/36 = 50.00%	Fixed source-state sensitivity
Convert guide nominal APL loads	11 / 55	27/55 = 49.09%	Post-result unit-reconciliation diagnostic
Interval-involving positive-width pairs	14 / 24	3 robustly ordered; 21 ambiguous	Cartesian outer sets; no endpoint covariance
Other interval-involving intersections	14 / 12	11 empty; 1 singleton	No interval order established

The five family deletions yield 1/10 crossings after removing the APL block, 18/36 after removing the Yin study, 27/45 after removing TLS-01, 27/45 after removing IGG-01, and 21/45 after removing KLS-1. The resulting 10.00-60.00% range is wide because these are composition changes to a small library. In particular, removing six related rows leaves only five rows and ten pairs. This source dependence is a central result, rather than a reason to average the five deletion fractions into another preferred estimate.

The additional 36 comparisons involving at least one ranged entry contain 24 positive-width intersections, 11 empty intersections and one singleton. Of the 24 positive-width cases, only three are robustly ordered under the rectangular outer sets; the other 21 remain ambiguous, and none has a forced crossing. The singleton compares KLS-1 with EAC-1A at 10 kPa and establishes only a conditional endpoint inequality. Recording it as stable ordering over a stress interval would add information that the supports do not contain.

The unit-reconciliation diagnostic changes one primary classification. The archive gives 23-143 kPa for the APL rows, whereas the guide describes nominal loads of 500, 1,500 and 3,000 pounds per square foot (Slabic et al., 2024). Converting the nominal end loads gives approximately 23.940-143.641 kPa. The CSM-LHT-1/OPRL2N crossing at 23.339 kPa then lies below the common support, reducing the crossing count to 27/55. Exact unit conversion does not make the underlying applied loads exact measurements. The diagnostic exposes a boundary sensitive to source precision; it does not replace the frozen literal-table analysis with a selected favorable result. Measurement terminology requires separating such representational precision from an established measurement uncertainty (JCGM, 2012).

Discussion

The analysis establishes that a single scalar ordering is not identified for many pairs of published parameter lines over their stated support. That conclusion follows from the model form, but the number of crossings, their stress locations and their concentration within source families are empirical properties of this compilation. A cohesion ranking alone emphasizes the intercept at zero normal stress, which may lie outside both reported test intervals. A friction-angle ranking emphasizes the line slope. Neither substitutes for checking the actual interval where the two representations can be compared.

The finite result also limits its own apparent strength. The fraction near one half should not be treated as a general frequency for lunar simulants: the library is selected, the parameter rows are heterogeneous, and the family deletion result shows substantial dependence on one assessment. Six different material names do not create six independent laboratory programs. Similarly, the near equality of the complete and residual-excluded crossing fractions does not demonstrate equivalence between peak and residual strength. It merely records what this particular exclusion does to this particular summary.

The ranged results show a second limitation of convenient table operations. Replacing each range with a midpoint would manufacture a scalar pairing and a unique line, even though ranges may summarize different densities, loads or test states. Our outer envelopes are deliberately permissive. If robust order fails in that enlarged set, the available fields alone do not determine it. This does not prove that every opposite order is experimentally realizable. Recovering joint coefficient pairs and their associated conditions could sharply reduce ambiguity, and recovering raw stress-shear measurements could permit a different analysis entirely. The present files support neither step.

Source auditing matters even when arithmetic is simple. The NASA guide resolves an otherwise uninformative OB-1A link, and its nominal loads reveal a classification sensitive to an approximate lower limit. The source year and abbreviated author order for TLS-01 also differ from the official conference record, which lists the full authors and a 2021 publication (Seehanam et al., 2021). We keep that bibliographic distinction visible. These examples caution against assuming that a downloadable table has eliminated interpretation and transcription issues. They also explain why independent algebraic agreement cannot certify original experimental provenance.

For lunar-domain information use, a useful input is therefore more than a pair of numbers and a material label. The method, stress range, state designation and distinction between scalar estimates and unpaired ranges determine which comparisons the representation permits. In the collection or navigation contexts discussed above, those conditions can delimit the physical statements available to a reasoning task. They provide no evidence about whether that model notices the limitations, chooses a suitable action, or outperforms another system. Those would require an explicitly designed model evaluation and are outside this study.

Computational reproducibility was handled by preserving source bytes, a frozen plan, all audited rows and every eligible pair. This follows the practical separation between computational records and the scientific interpretation of those records (Sandve et al., 2013). Scientific Agent Skills supplied procedural guidance for manuscript preparation and analysis reporting (Kassis et al., 2026); its use does not constitute a mechanical test, source endorsement or accountable-author approval. An independent implementation reparsed the original CSV and used separate Decimal coefficient algebra with the standard-library tangent, rather than the primary NumPy endpoint interpolation. All 55 classifications agreed, with maximum crossing-root difference below four times ten to the power of minus thirteen kPa. That agreement verifies the implemented arithmetic within the stated representation.

Conclusion

The archived simulant table supports 11 scalar direct-shear lines and 55 conditional pair comparisons, including 28 interior crossings under its literal stress limits. Source-family deletion and a nominal-load conversion show why neither that fraction nor every boundary classification should be generalized beyond the release. Ranged coefficients add substantial unresolved ordering and incomplete common support. The defensible output is a set of conditional comparisons with their missing information, rather than a universal material ranking or a claim about lunar engineering performance.

Data, code and review status

The source archive is identified by DOI, release, original filename and checksums in the source record. Article-specific files provide the complete 26-row audit, 55 scalar comparisons, 91 direct-shear pair records, source deletions and the nominal-load diagnostic. The result JSON stores the actual-byte SHA256 of the primary CSV. Accountable-author review, human source-claim verification, conflict-of-interest confirmation and submission approval remain PENDING. This draft reports a secondary computational analysis of public compiled values, with no new mechanical experiments or model inference runs.

References

1. Ryu, Byung-Hyun; Wang, Cheng-Can; Chang, Ilhan. (2018). Development and Geotechnical Engineering Properties of KLS-1 Lunar Simulant. Journal of Aerospace Engineering. https://doi.org/10.1061/(asce)as.1943-5525.0000798
2. Zou, Yuan; Wu, Huanyu; Chai, Shupeng; Yang, Wei; Ruan, Renhao; Zhao, Qi. (2024). Development and characterization of the PolyU-1 lunar regolith simulant based on Chang'e-5 returned samples. International Journal of Mining Science and Technology. https://doi.org/10.1016/j.ijmst.2024.08.006
3. Rowe, P. W.. (1962). The stress-dilatancy relation for static equilibrium of an assembly of particles in contact. Proceedings of the Royal Society of London. Series A. Mathematical and Physical Sciences. https://doi.org/10.1098/rspa.1962.0193
4. Terzaghi, Karl. (1943). Theoretical Soil Mechanics. Wiley. https://doi.org/10.1002/9780470172766
5. Mitchell, James K.; Soga, Kenichi; O'Sullivan, Catherine. (2025). Fundamentals of Soil Behavior. Wiley. https://doi.org/10.1002/9781119832348
6. Xiao, Xin-Yu; Tian, Ye; He, Zhixian; Chen, Qilin; Wang, Shiqi; Xia, Qianchen. (2026). Lunar-R1: Towards Efficient Reasoning of Large Language Models for Lunar Exploration via Reinforcement Learning. Proceedings of the 2026 Conference on Empirical Methods in Natural Language Processing: Industry Track. https://aclanthology.org/2026.emnlp-industry.5/.
7. Saltelli, Andrea; Ratto, Marco; Andres, Terry; Campolongo, Francesca; Cariboni, Jessica; Gatelli, Debora; Saisana, Michaela; Tarantola, Stefano. (2008). Global Sensitivity Analysis. The Primer. Wiley. https://doi.org/10.1002/9780470725184
8. Been, K.; Jefferies, M. G.. (1985). A state parameter for sands. Géotechnique. https://doi.org/10.1680/geot.1985.35.2.99
9. Joint Committee for Guides in Metrology. (2012). International vocabulary of metrology - Basic and general concepts and associated terms (VIM), third edition (JCGM200:2012). Bureau International des Poids et Mesures. https://doi.org/10.59161/JCGM200-2012
10. Alshibli, Khalid A.; Hasan, Alsidqi. (2009). Strength Properties of JSC-1A Lunar Regolith Simulant. Journal of Geotechnical and Geoenvironmental Engineering. https://doi.org/10.1061/(asce)gt.1943-5606.0000068
11. Sandve, Geir Kjetil; Nekrutenko, Anton; Taylor, James; Hovig, Eivind. (2013). Ten Simple Rules for Reproducible Computational Research. PLoS Computational Biology. https://doi.org/10.1371/journal.pcbi.1003285
12. Teng, Yue; Wang, Shun; Cui, Yifei; Pang, Yong. (2025). Influence of loading conditions on mechanical behaviors of lunar regolith simulant WHU-1 based on Chang'e-5 returned samples. Acta Geotechnica. https://doi.org/10.1007/s11440-025-02553-7
13. Schanz, T.; Vermeer, P. A.. (1996). Angles of friction and dilatancy of sand. Géotechnique. https://doi.org/10.1680/geot.1996.46.1.145

14. Phoon, Kok-Kwang; Kulhawy, Fred H. (1999). Characterization of geotechnical variability. Canadian Geotechnical Journal. https://doi.org/10.1139/t99-038

15. Yin, Kexin; Cheng, Zhichao; Liu, Jiangxin; Chen, An. (2023). Shear properties of LHS-1 and LMS-1 Lunar regolith simulants. Planetary and Space Science. https://doi.org/10.1016/j.pss.2022.105630

16. Suescun-Florez, Eduardo; Roslyakov, Stanislav; Iskander, Magued; Baamer, Mohammed. (2015). Geotechnical Properties of BP-1 Lunar Regolith Simulant. Journal of Aerospace Engineering. https://doi.org/10.1061/(asce)as.1943-5525.0000462

17. Baecher, Gregory B.; Christian, John T.. (2003). Reliability and Statistics in Geotechnical Engineering. Wiley. https://www.wiley.com/en-gb/reliability-and-statistics-in-geotechnical-engineering-p-9780471498339

18. Slabic, Ane; Gruener, John E.; Kovtun, Rostislav N.; Rickman, Douglas L.; Sibille, Laurent; Oravec, Heather A.; Edmunson, Jennifer; Keprta, Sean. (2024). Lunar Regolith Simulant User's Guide: Revision A. NASA/TM-20240011783. https://ntrs.nasa.gov/citations/20240011783

19. Ruan, Renhao; Yang, Wei; Zhang, Di; Tian, Heng-Ci; Zhao, Qi; Zou, Yuan; Yu, Bin. (2024). A moderate-Ti lunar mare soil simulant: IGG-01. Acta Astronautica. https://doi.org/10.1016/j.actaastro.2024.08.010

20. Duncan, J. Michael; Wright, Stephen G.; Brandon, Thomas L.. (2014). Soil Strength and Slope Stability, second edition. Wiley. https://www.wiley.com/en-ca/soil-strength-and-slope-stability-2nd-edition-p-9781118917961

21. Wood, David Muir. (1991). Soil Behaviour and Critical State Soil Mechanics. Cambridge University Press. https://doi.org/10.1017/cbo9781139878272

22. Gasteiner, Léonie; Murdoch, Naomi; D'Angelo, Olfa. (2026a). An Open Database of Lunar Regolith and Simulants Properties. International Journal for Numerical and Analytical Methods in Geomechanics. https://doi.org/10.1002/nag.70432

23. Seehanam, Saran; Santironnarong, Siraphob; Meesuay, Wasin; Soralump, Suttisak; Thowiwat, Worawat; Jitklongsub, Sarinya; Chancharoen, Wares. (2021). Development and Mechanical properties of the first Thailand lunar regolith simulant (TLS-01). Proceedings of Innovation Aviation & Aerospace Industry - International Conference 2021. https://sciforum.net/paper/10583

24. Bolton, M. D.. (1986). The strength and dilatancy of sands. Géotechnique. https://doi.org/10.1680/geot.1986.36.1.65

25. Gasteiner, Léonie; Murdoch, Naomi; D'Angelo, Olfa. (2026b). Dataset for the Lunar Regolith Database, version 3.0. Recherche Data Gouv. https://doi.org/10.57745/NTSZ8G

26. Kassis, Timothy; Agarwal, Vinayak; He, Yuhuan; Patel, Darshil; Brueckner, Aubrey M.. (2026). Scientific Agent Skills: A Library of Procedural Knowledge for Research Agents. arXiv preprint. https://arxiv.org/abs/2609.00065

27. Drucker, D. C.; Prager, W.. (1952). Soil mechanics and plastic analysis or limit design. Quarterly of Applied Mathematics. https://doi.org/10.1090/qam/48291.

28. Thornton, C.. (2000). Numerical simulations of deviatoric shear deformation of granular media. Géotechnique. https://doi.org/10.1680/geot.2000.50.1.43

29. Cundall, P. A.; Strack, O. D. L.. (1979). A discrete numerical model for granular assemblies. Géotechnique. https://doi.org/10.1680/geot.1979.29.1.47

30. Manski, Charles F.. (2003). Partial Identification of Probability Distributions. Springer Series in Statistics. https://doi.org/10.1007/b97478